EMORY LIBRARIES & INFORMATION TECHNOLOGY | OpenEmory

The 3.2 angstrom structure of a bioengineered variant of blood coagulation factor VIII indicates two conformations of the C2 domain

Ian W. Smith, *Western Washington University*
Anne E. d'Aquino, *Western Washington University*
Christopher W. Coyle, *Emory University*
Andrew Fedanov, *Emory University*
Ernest T. Parker, *Emory University*
Gabriela Denning, *Expression Therapeutics, LLC.*
H Trent Spencer, *Emory University*
John Lollar, *Emory University*
Christopher Doering, *Emory University*
P. Clint Spiegel. Jr., *Western Washington University*

Journal Title: JOURNAL OF THROMBOSIS AND HAEMOSTASIS

Volume: Volume 18, Number 1

Publisher: WILEY | 2019-09-08, Pages 57-69

Type of Work: Article | Post-print: After Peer Review

Publisher DOI: 10.1111/jth.14621

Permanent URL: https://pid.emory.edu/ark:/25593/vrpgc

Final published version: http://dx.doi.org/10.1111/jth.14621

Copyright information:

2019

Accessed April 21, 2025 1:21 AM EDT

Author Manuscript

Author Manuscript

Author Manuscript

Author Manuscript

HHS Public Access

Author manuscript

J Thromb Haemost. Author manuscript; available in PMC 2021 January 01.

Published in final edited form as:

J Thromb Haemost. 2020 January ; 18(1): 57–69. doi:10.1111/jth.14621.

The 3.2 Å Structure of a Bioengineered Variant of Blood Coagulation Factor VIII Indicates Two Conformations of the C2 Domain

Ian W. Smith[1], **Anne E. d'Aquino**[1], **Christopher W. Coyle**[2], **Andrew Fedanov**[3], **Ernest T. Parker**[3], **Gabriela Denning**[4], **H. Trent Spencer**[3], **Pete Lollar**[3], **Christopher B. Doering**[3], **P. Clint Spiegel Jr.**[1,*]

[1]Department of Chemistry, Western Washington University, 516 High Street, MS 9150, Bellingham, WA 98225-9150

[2]Graduate Program in Molecular and Systems Pharmacology, Graduate Division of Biological and Biomedical Sciences, Laney Graduate School, Emory University, Atlanta, GA 30322

[3]Aflac Cancer and Blood Disorders Center, Department of Pediatrics, Emory University, Atlanta, GA 30322

[4]Expression Therapeutics, LLC. Tucker, GA 30084

Abstract

Background: Coagulation factor VIII represents one of the oldest protein-based therapeutics, serving as an effective hemophilia A treatment for half a century. Optimal treatment consists of repeated intravenous infusions of blood coagulation factor VIII (FVIII) per week for life. Despite overall treatment success, significant limitations remain including treatment invasiveness, duration, immunogenicity, and cost. These issues have inspired research into the development of bioengineered FVIII products and gene therapies.

Objectives: To structurally characterize a bioengineered construct of FVIII, termed ET3i, which is a human/porcine chimeric B domain-deleted heterodimer with improved expression and slower A2 domain dissociation following proteolytic activation by thrombin.

Methods: The structure of ET3i was characterized with X-ray crystallography and tandem mass spectrometry-based glycoproteomics.

*To whom correspondence should be addressed: 1-360-650-3137 phone, 1-360-650-2826 fax, Paul.Spiegel@wwu.edu.

Author Contributions

IWS and AED planned experiments, performed experiments, analyzed data, and assisted in writing the paper. ETP, CWC and AF performed experiments and analyzed data. GD, HTS and PL planned experiments, analyzed data and edited the paper. CBD planned experiments, performed experiments, analyzed data, and edited the paper. PCS planned experiments, analyzed data and wrote the paper.

Authorship and conflict-of-interest statements

P.L. is inventor on a patent application describing ET3i and is an inventor on patents owned by Emory University claiming compositions of matter that include modified FVIII proteins with reduced reactivity with anti-FVIII antibodies. C.B.D., P.L. and H.T.S. are co-founders of Expression Therapeutics and own equity in the company. Expression Therapeutics owns the intellectual property associated with ET3i. G.D. is an employee of Expression Therapeutics and owns equity in the company. The terms of this arrangement have been reviewed and approved by Emory University in accordance with its conflict of interest policies.

Author Manuscript Author Manuscript Author Manuscript Author Manuscript

Results: Here, we report the 3.2 Å crystal structure of ET3i and characterize the distribution of N-linked glycans with LC-MS/MS glycoproteomics. This structure shows remarkable conservation with the human FVIII protein and provides a detailed view of the interface between the A2 domain and the remaining FVIII structure. With two FVIII molecules in the crystal, we observe two conformations of the C2 domain relative to the remaining FVIII structure. The improved model and stereochemistry of ET3i served as a scaffold to generate an improved, refined structure of human FVIII. With the original datasets at 3.7 Å and 4.0 Å resolution, this new structure resulted in improved refinement statistics.

Conclusions: These improved structures yield a more confident model for next generation engineering efforts to develop FVIII therapeutics with longer half-lives, higher expression levels and lower immunogenicity.

Keywords

factor VIII; blood coagulation; x-ray crystallography

Introduction

Hemophilia A is an X-linked bleeding disorder caused by deficiency of blood coagulation factor VIII (FVIII), which affects 1 in 5,000 males worldwide. FVIII is required for formation of stable blood clots and FVIII deficiency results in uncontrolled bleeding.[1] Following proteolytic activation, FVIIIa serves as a non-enzymatic protein cofactor for the serine protease factor IXa (FIXa) and is essential for the intrinsic pathway of the blood coagulation cascade.[1,2] The presence of FVIII upregulates the activity of FIXa in the intrinsic tenase complex, which proteolytically activates factor X (FX) to activated factor X (FXa), by approximately 200,000-fold.[3] FVIII is expressed as a 2,332-residue glycoprotein with the domain sequence of A1-A2-B-*ap*-A3-C1-C2.[4] Prior to secretion, single-chain FVIII is cleaved at R1648 at the COOH-terminus of the B domain, and undergoes incomplete proteolytic processing at residues R740 at the COOH-terminus of the A2 domain and residues R817, R1115, and R1313 in the B domain.[5] Differential processing partially removes the B domain and results in a population of mature FVIII heterodimers with the domain sequence of A1-A2-B'/*ap*-A3-C1-C2.[4,6] Heterodimeric FVIII circulates in a tightly bound complex with von Willebrand factor (VWF), which increases the circulatory half-life of FVIII and shields it from clearance receptors.[7,8]

Following vascular injury, VWF is hypothesized to bind activated platelet surfaces expressing the glycoprotein Ib-IX (GpIb/IX) receptor, potentially localizing the VWF:FVIII complex to the site of hemostasis.[9] While bound to VWF, FVIII is proteolytically cleaved by thrombin or FXa at residues R372, R740 and R1689, leading to dissociation from VWF and formation of an activated FVIII heterotrimer (FVIIIa) with the domain structure A1/A2/A3-C1-C2.[10,11] Specifically, cleavages at R372 and R1689 lead to emergence of FIXa cofactor activity and dissociation from VWF, respectively.[7,12–15] The FVIII C1 and C2 domains contain a dense arrangement of basic, positively-charged amino acid residues that are proximal to protruding beta-hairpin turns that contain solvent-exposed hydrophobic patches, allowing FVIIIa to bind to negatively-charged, phosphatidylserine-containing activated platelet surfaces.[16–23] Previous electron microscopic and modeling results have suggested

Author Manuscript Author Manuscript Author Manuscript Author Manuscript

large-scale conformational changes for the C domains upon membrane binding whereby the C domains either tilt relative to the trimeric A domain assembly or the C2 domain protrudes outward in an extended structure (Figure S1).[24–27]

The established current treatment for hemophilia A is regular infusions of FVIII to restore clotting capability, commonly termed “factor VIII replacement therapy”.[28] Approximately 30% of hemophilia A patients receiving FVIII replacement, either from plasma-derived or recombinant sources, develop an anti-FVIII immune response, which results in the development of pathogenic inhibitory antibodies, or “inhibitors”.[29–31] Anti-FVIII inhibitors represent a major treatment complication, reducing the efficacy of FVIII.[32] Additionally, FVIII inhibitors can develop as an autoimmune event in individuals who do not have congenital hemophilia A, producing a condition called acquired hemophilia A. One treatment for inhibitor development employs Immune Tolerance Induction (ITI), a regimen of frequent, high dosage infusions of FVIII.[33] Although the mechanism of action of ITI is unknown, it is effective in eradicating inhibitors in 70% of cases. However, the cost and quantity of FVIII product required makes ITI inaccessible to most of the global population.

Interspecies variability in protein expression/secretion, specific activity, antigenicity, immunogenicity and stability have been previously observed for FVIII preparations from different species.[34–36] For example, porcine FVIII (pFVIII) possesses increased specific activity and stability following activation by thrombin.[37,38] The latter observation correlates with an increased affinity of the A2 domain in the heterotrimeric FVIIIa state, predominantly due to a three-fold decrease in the dissociation rate constant.[18] Additionally, it has been demonstrated that recombinant B-domain-deleted (BDD) pFVIII expresses at 10- to 14-fold higher levels than recombinant hFVIII.[35] The decreased antigenicity profile of recombinant BDD pFVIII has led to its approval for use in patients with acquired hemophilia A (Obizur).[39] Novel human/porcine chimeric FVIII constructs have also been created to identify the domains responsible for contributing increased expression and stability of pFVIII.[40] The chimeric construct, designated “ET3i” (previously denoted as HP47), containing the porcine A1 and A3 domains, demonstrates higher expression and activity levels than recombinant human FVIII (hFVIII) in *in vitro* and *in vivo* expression systems such as those used for recombinant FVIII manufacturing and clinical gene therapy, respectively.[40–46] This expression differential was shown to be the result of reduced interaction with unfolded protein response chaperones in the endoplasmic reticulum.[47]

In this study, we report the refined molecular structure of the ET3i human/porcine chimeric FVIII construct at 3.2 Å, the highest resolution structure of FVIII communicated to date. Previously published FVIII structures are intrinsically low resolution (3.7–4.2 Å), in the same crystallographic space group and contain inconsistencies (PDB codes: 2R7E, 3CDZ, 5K8D, and 4BDV).[21,24,48] Additionally, the human/porcine chimera provides insight to the inter-domain surface contact residues that may contribute to the differential stability of human and porcine FVIII proteins. Furthermore, a novel conformational domain movement is observed between the C2 domains of the two ET3i molecules in the crystallographic asymmetric unit (ASU). Based on the role of the C2 domain in binding to phosphatidylserine-rich activated platelet surfaces, this observed conformational movement could have physiological implications to the membrane binding of FVIII.

Author Manuscript Author Manuscript Author Manuscript Author Manuscript

Materials and Methods

Production of ET3i

The BDD human/porcine chimeric FVIII construct ET3i was expressed and purified as previously described.[45] Protein production for crystallographic studies was performed in baby hamster kidney-derived cells as previously described.[44] The purified ET3i was subsequently stored in a 0.35 mM NaCl solution at 0.84 mg/mL at – 80 °C. The LC-ESI-MS/MS glycosylation characterization of ET3i was performed by the University of Georgia Complex Carbohydrates Research Center (https://ast.uga.edu/glycoproteomics/).

Crystallization and Structure Determination

ET3i crystals of sufficient size and quality for X-ray diffraction and crystallographic structure determination were grown by hanging drop vapor diffusion in a 2:1 ratio of 0.84 mg/mL ET3i protein (0.35 mM NaCl) and a crystallization solution containing 26% (w/v) polyethylene glycol (PEG) 3350, 25 mmol/L $MgCl_2$, and 25 mmol/L HEPES (pH 8.3). Crystals appeared at room temperature over several days and were cryoprotected in the same crystallization solution containing 30% (v/v) glycerol. X-ray diffraction data were collected on the Advanced Light Source (ALS) SIBYLS beamline 12.3.1 at the Lawrence Berkeley National Laboratory (Berkeley, CA). X-ray diffraction data collection, indexing, and scaling were accomplished with Adxv, XDS and CCP4.[49] Phases were computationally resolved by molecular replacement using the 3.7 Å molecular model of human factor VIII (PDB: 2R7E) as a starting model with PHASER-MR.[50] Model building and refinement were completed with Coot and PHENIX, respectively.[51] Surface electrostatic calculations were performed with APBS,[52] and docking simulations were done with RosettaDock on the ROSIE server.[53] All figure representations were generated with The PyMOL Molecular Graphics System, Version 2.0 (Schrödinger, LLC). The X-ray crystal structures of ET3i and improved human FVIII have been deposited in the Protein Databank with the accession codes 6MF0 and 6MF2, respectively.

Results

Overall Structure of ET3i

The crystal structure of ET3i reveals a trimeric A domain structure containing the porcine A1 and A3 domains and human A2 domain (Figures 1A, 1B; Table 1). The structure possesses three glycosylation sites at residues N240, N1810, and N2118 and three metal ions embedded within the A domain trimeric assembly (Figure 1A). Two copies of ET3i are present in the crystallographic ASU, allowing for two models (A and B) within the same crystal (Figure 1C). Model A superimposes with the previous highest resolution structure (pdb#: 2R7E)[21] with an RMSD of 1.213 Å (Figure 1D).

The three metal coordination sites observed in ET3i can be interpreted in light of recent X-ray fluorescence analysis, colorimetric analysis and X-ray crystallography of the recombinant BDD hFVIII molecule turoctocog alfa by Svennson et al. (Figures 1A, S2).[21,24,48] Their results were consistent with single Zn^{2+} and Cu^{+} sites in the A1 and A3 domains, respectively. The identification of cuprous (Cu^{+}) ion is consistent with the

Author Manuscript Author Manuscript Author Manuscript Author Manuscript

observation that one molar equivalent of cuprous (Cu^{+}), but not cupric (Cu^{2+}), ion could reconstitute EDTA-inactivated FVIII.[54] By contrast, in previous crystallographic models of human fVIII, Cu^{2+} was modeled into the A1 and A3 domain sites. In our model, the A1 domain Zn^{2+} is coordinated by H268, C311, H318, and potentially H233 (Figure S2B). This modeling is markedly unique relative to previous structures, as the original modeling suggested H316 instead of H318 (H315 and H317 in human sequence, respectively), but this previously reported orientation was not supported by the electron density. The A3 domain Cu^{+} binding site is coordinated by residues H1954, C2000, and H2005, with the neighboring M2010 nearby (Figure S2C).

In the ET3i structure, N-linked glycans were modeled at residues N240 (N-NAG-NAG-MAN_3), N1810 (Chain A: N-NAG-NAG-MAN; Chain B: N-NAG(FUC)-NAG-MAN_3-NAG), and N2118 (Chain A: N-NAG-NAG-MAN_4; Chain B: N-NAG-NAG-MAN_3) based on observable electron density (Figure 1A). The hFVIII residue N41 is a glycine in ET3i due to the A1 pFVIII sequence, thus no glycosylation was expected or observed. In the ET3i model B, N1810 was the only site where fucosylation and a terminal NAG residue was observed. To obtain more detailed information on ET3i glycation, glycoproteomics analysis and glycoform quantification were performed using LC-MS/MS. A broad distribution of complex, hybrid and high mannose glycans was identified and localized to N214, N240, N1810 and N2118 (Supplementary Data). Similar to human FVIII, the sequence predicted N582 site was not occupied. Although the many glycoforms were identified at each position, the intra-site conservation between ET3i and commercial human FVIII glycoforms was similar to that reported by Canis et al.[55]

Interfacial Interactions of the FVIII A Domains

Upon inspection of the ET3i and hFVIII sequence differences that occur in the A1 and A3 domains, most occur at the solvent-accessible surface (Figure 2A), and the majority of the species-specific sequence differences arise in the A1 domain. The observation that there is a relative dearth of sequence differences that are present at the A2 interface with both the A1 and A3 domains is unexpected (Figure 2A), as the presence of pFVIII sequences in the A1 and A3 domains is concomitant with a decreased A2 domain dissociation rate constant.[56] Given the sequence conservation at the A2 domain interface, the higher resolution of the ET3i structure allows for a comprehensive description of the residue-specific interactions that occur between the A2 domain and the A1 and A3 domains (Figures 2B, 2C, Tables S1, S2). Here, the interface between A2 and the remaining FVIII structure is notably polar, possibly contributing to its intrinsically fast dissociation rate constant despite significant buried surface area (874 $Å^2$ and 854 $Å^2$ for the A1–A2 and A2–A3 domain interfaces, respectively). In contrast to the conservation of the A2 domain interface, there are several sequence differences that occur at the A1–A3 domain interface (Figures 2D, 2E). The A1 domain harbors seven residues that are different between hFVIII and ET3i while the A3 domain has four directly at the A1–A3 interface.

The effect of stability of the A2 domain on the cofactor activity of FVIII has been extensively characterized through both querying the hemophilia A mutational database and protein engineering efforts. Hemophilia A mutations that are characterized as having a

Author Manuscript Author Manuscript Author Manuscript Author Manuscript

higher activity measured through a one-stage clotting assay versus a two-stage clotting assay were previously suggested to be the result of an increased rate of A2 domain dissociation.[57] Highlighting these hemophilia A-associated mutations localizes the majority of them to the A2 domain interface with both the A1 and A3 domains, with additional mutations also occurring at the A1–A3 interface and two on the distal face of the A3 domain (Figure 3A). Previous protein engineering efforts have shown an increase in FVIII cofactor activity when introducing hydrophobic residues (D519V/E665V and E1984A,V/E665I), which are present at the A2 domain interface (Figures 3A, 3C).[58,59] Furthermore, introduction of cysteine residues at the A2 interface to form disulfide bonds have also demonstrated a decreased A2 dissociation rate constant (H282C/S524C, M662/D1828, Y664/T1826, and D666/S1788).[60–62] The ET3i structure indicates that the C_β-C_β distances for these residue pairs are between 5 and 7.5 Å, consistent with the feasibility of forming disulfide bonds (Figure 3B). Lastly, the mutation Q316H in hFVIII results in a decreased A2 dissociation rate constant, which is the homologous porcine residue (shown as H317 in the ET3i structure).[63] While this residue does not make direct contact with the A2 domain, it folds back to H-bond with main chain carbonyl oxygen of A231, which may stabilize a direct salt bridge between the preceding histidine with E540 of the A2 domain (Figure 3D).

C2 Domain Conformational Changes

Previous crystal structures of FVIII, including the model A of the ET3i structure, adopt similar conformations of the C2 domain relative to the remaining FVIII structure, which is also similar to the orientation of the C2 domain in the activated protein C-inactivated factor Va (FVai) structure.[64] In model B of the ET3i structure, we observe a new conformation of the C2 domain relative to the domain arrangement of the remaining FVIII structure (Figure 4A). This new conformation consists of a rotation and tilt about a central set of core residues that do not deviate significantly in cartesian space when non-crystallographic symmetry metrics are compared between models A and B of the ET3i structure. This conformational change results in a rotation about a central axis by approximately 35–45° and movements of individual residues by as much as 14 Å (Figure 4A).

Upon modeling the C1 domain in its putative membrane-binding orientation, which is based on homology to our previously proposed docking of the homologous C2 domain using high resolution crystal structures, electrostatic calculations and antibody inhibitor epitopes that block membrane binding,[16,22,23] we observe differences between membrane docking orientations for the A and B models of FVIII. With the C1 domain initially docked to a membrane plane, we observe two distinct conformations of the C2 domain, which may represent a second kinetic step of membrane association in accordance with previous studies (Figure 4B).[18,65,66] If initial membrane binding by the C2 domain is assumed, the movement from the A model to the B model conformations adjust the C1 domain from an ‘undocked’ conformation (where a plane cannot be drawn between each C domain for membrane binding) to a ‘docked’ conformation that places each C domain in a similar orientation with respect to a putative membrane surface (Figure S5). The novel orientation of the C2 domain relative to FVIII is not due to a loss of interdomain interactions, but a shift of specific contacts between the C2 and A1 domains that stabilize both conformations (Figure 4C). Lastly, the projection of FVIII upward by approximately 70° relative to the membrane plane

Author Manuscript Author Manuscript Author Manuscript Author Manuscript

is consistent with previous FRET data indicating the FIXa active site should be 75–90 Å above the membrane as well as recent single molecule AFM studies.[67,68]

Refinement of an Improved Human FVIII Structure

The two original structures of hFVIII were published at similar resolutions (3.7 and 4.0 Å for Protein Databank entries 2R7E and 3CDZ, respectively),[21,24] in the same crystallographic space group with similar unit cell dimensions, and resulted in very similar overall structures. However, there are significant differences between the models within the A2 domain. In particular, the amino acid chain register and placement within the core of the protein fold deviates significantly. With the improved resolution of the ET3i FVIII structure, a new model of hFVIII was built and refined to reconcile these differences. Here, we mutated the ET3i structure to hFVIII and phased both previous hFVIII X-ray datasets with our ET3i-derived model of hFVIII. The datasets were refined against the original structure factors that were directly downloaded from the Protein Databank, which preserves the original R_{free}-flagged reflections that were used in our refinement. Both previous hFVIII structures were incorrectly modeled in the 644–649 loop (Figures 5A, 5B), with the 2R7E structure being out of register by one residue following the loop (Figure 5B). Additionally, the 652–657 loop was also mismodeled in the 2R7E structure, ultimately resulting in the original FVIII structure being out of register by two residues, which propagates throughout the remainder of the A2 domain to residue 711 (Figure 5C). The density features in the new hFVIII model strongly suggest the presence of only one Ca^{2+} ion (the 2R7E model contains two) and the remaining bound metal ions were also modeled as in the ET3i structure to be consistent with previous findings to include one each of Cu^{+} and Zn^{2+} ions (original structures contained two Cu^{2+}).[48] We also find that the hFVIII structure resulted in better density features and refinement values when the Zn^{2+} coordination site is modeled with H317 as opposed to the original modeling with H315 (Figure 3D). Following the building and refinement of the hFVIII with both the 2R7E and 3CDZ datasets, the resultant structure was highly homologous to the ET3i model A (0.837 Å RMSD) (Figure 5D). Lastly, the final refinement values for both crystallographic datasets (2R7E and 3CDZ) significantly improved with our new model of hFVIII (Table 2).

Discussion

FVIII-based bioengineering efforts have advanced innovative therapeutic strategies over the past 10 years. FVIII derived from other species (ovine, murine, porcine) as well as ancestral reconstructions have demonstrated a potential for the development of more effective FVIII products possessing improved specific activity, expression levels, A2 dissociation kinetics, antigenicity and immunogenicity.[34–36,46] Recent efforts have resulted in the generation of a recombinant pFVIII product, which is now clinically approved (Obizur).[39] ET3i and ET3 represent a bioengineered recombinant FVIII and a gene therapy transgene, respectively, under development for the control and prevention of bleeding, immune tolerance induction and gene therapy of hemophilia A.[43–45] ET3i, which harbors porcine sequences within the A1 and A3 domains while the A2, C1 and C2 domains are human, displays 4 of the 5 design improvements, while the immunogenicity was shown to be indistinguishable to recombinant BDD human FVIII in a murine hemophilia A model.[43,45,56]

Author Manuscript Author Manuscript Author Manuscript Author Manuscript

Moreover, the improved resolution of ET3i allows for newly refined structure of hFVIII (Figure 5D). Following a complete characterization of the N-linked glycans present within ET3i with LC-MS/MS, we modeled each of three glycosylation sites within the limits of the observed electron density as well as modeled the three conserved metal binding sites (Figure S2). Strikingly, the A2 interface with the A1 and A3 domains is highly conserved, which is in contrast to the interface between A1 and A3 that harbors several amino acid substitutions between the human and porcine sequences (Figure 2). Previous studies have indicated that the C-terminal cupredoxin-like subdomain of A1 is responsible for improved A2 domain dissociation kinetics and stability, and this region forms the majority of the A1–A3 interface.[56] Thus, we hypothesize that the increase in A2 domain stability, as well as expression, of pFVIIIa and ET3i, may be due to an increase in the stability of the interface between A1 and A3, which would indirectly affect the A2 binding interface and possibly reduce interaction with the unfolded protein response pathway. Regarding the latter, both A1 and A3 domain porcine sequence were found to be necessary and sufficient for increased secretion efficiency.[40] Additionally, the Q316H substitution within the A2 domain also contributes to improved A2 dissociation kinetics, which appears to play a more direct role in A2 binding (Figure 3D).[63]

Contrasting the structure of ET3i with mutations associated with hemophilia A is a powerful mechanism by which to rationalize the effect of certain point mutations on the cofactor activity of FVIII as well as inform protein engineering efforts. Previous studies of hemophilia A mutations that lower activity in two-stage versus one-stage clotting assays were shown to result from an increased rate of A2 dissociation following activation.[57,69] Here, we modeled these mutations onto the structure of ET3i to illustrate that most of them occur at the A2 domain interface while some were also localized to either the A1–A3 interface or to the distal side of the A3 domain (Figure 3A). Moreover, engineered amino acid alterations to introduce increased hydrophobicity or disulfide bonds to stabilize the A2 domain interface are also highlighted within the ET3i structure to inform further engineering efforts (Figures 3B, 3C).[58–62] In addition, the ET3i structure allows for a comprehensive description of immunodominant inhibitory epitopes in both the A2 domain (Figure S3) and the C1 domain (Figure S4).[70,71] The localization of the A2 domain epitopes further refines the understanding of which regions are responsible for the activity of the intrinsic FXase complex versus which are critical for thrombin-catalyzed FVIII activation and VWF dissociation.[71] Based on epitope mapping, it was shown that residues 604–711 block proteolytic cleavage at R372, R740 and R1689. Structural modeling of this peptide epitope indicates that a surface consisting of residues 626–637, 653–664, and 677–688 buttresses all three cleavage sites and resides on the membrane-proximal face of FVIII (Figure S3). By contrast, the peptide epitopes that inhibit FXa generation consist of 403–444 and 484–508. These two regions are close in space when reduced to 429–444 and 484–508 where they reside atop the A2 domain, adjacent to the loop cleaved at R372. The distances of these two loops to the planar membrane surface are consistent with previous FRET data concerning the distance of the FIXa active site to the membrane (85–100 Å for 429–444 and 90–100 Å for 484–508).[68] For anti-C1 domain inhibitor epitopes, structural modeling refines the regions of FVIII that bind VWF and PS, as well as how certain antibody binding results in allosteric H/D protection patterns (Figure S4).[70] The localization of the PS binding region of

Author Manuscript Author Manuscript Author Manuscript Author Manuscript

the C1 domain is consistent with previous structure-based models for C2 domain PS binding.[16,23] In this model of C2 domain binding to PS membranes, the bottom of the C2 domain fold possesses two β-hairpin loops with surface-exposed hydrophobic residues (M2199/F2200 and L2251/L2252) which are hypothesized to insert into the nonpolar interior of the membrane bilayer. The negative charge of the PS surface is then proposed to interact with a ring of positively-charged basic residues. The homologous C1 domain harbors all these same features, suggesting a similar mechanism of PS membrane binding.

The structure of ET3i is the result of a new crystal form, which contains two molecules of the ET3i structure in the asymmetric unit. The A model recapitulates the previously determined structures of hFVIII with respect to the domain architecture of the entire structure.[21,24] In contrast to this structural conservation, the B model indicates a new conformation of the C2 domain relative to the remaining structure of FVIII. The B model C2 domain rolls and tilts relative to the orientation present in the A model, which alters the projection of the FVIII structure with respect to a putative membrane-binding surface (Figure 4). This suggests a multi-phase membrane association through local conformational changes to the C2 domain relative to the remaining FVIII structure, as previously hypothesized.[24] It should be noted that the B model C2 domain makes unique crystal contacts that may stabilize its novel conformation, however, this must be relatively stable to be present in the crystal lattice in order to be observed. Additionally, the ET3i structure does contain porcine sequence in the A1 domain, but a single residue change (A109S) is proximal to the A1/C2 domain interface, which would unlikely result in a structural artifact. Alternatively, the observed conformational change of the C2 domain could represent the vWF-bound conformation whereby the vWF D’ domain binds along the C1 domain and additional interactions occur between the vWF D3 domain and the C2 domain.

This conformational change of the C2 domain observed at 3.2 Å resolution is markedly different from previous models based on lower resolution (15–20 Å) electron microscopic studies.[25–27] By contrast, these models suggest large-scale conformational changes to both C domains upon membrane binding to either PS-containing lipid nanodiscs or lipid nanotubes (Figure S1).[18,65–67,72] Based on rigid body modeling, the different cryoEM-based structures suggest a rotation of the C1 domain to form a new interdomain interface between the A3 and C1 domains of FVIII, projecting the β-hairpin loops upwards with respect to the C2 domain orientations. This allows the C2 domain to swing between the two cryoEM structures by over 90°, leading the authors to conclude that large-scale domain movements of the C2 domain occur upon PS membrane binding and are predominantly responsible for this interaction. While further experimental observations are necessary to support these models, they suggest that these changes in conformation of C2 likely occur following dissociation of FVIIIa from VWF, allowing it to bind activated platelet surfaces and serve as a cofactor for the FIXa-mediated intrinsic FXase reaction.

Finally, the improved resolution and corrected modeling of the FVIII structure allowed for more accurate electrostatic surface potential calculations. In doing so, a large basic surface is observed on the side of the C1 domain, including a cleft residing at the interface between the C1 and A3 domains (Figures 6A, 6B). Given that this region is hypothesized to bind the TIL’E’ domain of VWF based on both cryoEM reconstructions and H/D mass spectrometry

Author Manuscript Author Manuscript Author Manuscript Author Manuscript

data, we elected to perform docking simulations for this complex (Figure S6).[73,74] The TIL'E' domain has an acidic protrusion (Figure 6B),[75] which also possesses a surface that is complementary to the basic binding cleft on FVIII (Figure 6A). The resultant protein complex is consistent with previous H/D exchange data as well as hemophilia A- and von Willebrand Disease-associated mutations (Figure 6C).[73,75] Upon association of the VWF TIL'E' domain with the ET3i structure, it is also apparent that the basic binding cleft of the TIL'E' domain sits adjacent to the N-terminus of the A3 domain. In our modeling of the A3 domain, we were able to observe density for up to K1693, which is immediately C-terminal to the thrombin cleavage that occurs at R1689 to dissociate FVIIIa from VWF. This region N-terminal of the A3 domain is highly acidic and harbors a sulfated tyrosine at position 1680 that has been shown to be critical for FVIII cofactor function. We hypothesize that the acidic peptide, and likely the sulfated tyrosine, constitute a high affinity interaction between FVIII and VWF, and that cleavage of R1689 by thrombin removes this tether to allow FVIII to dissociate from VWF and subsequently bind to activated platelet surfaces to perform its essential cofactor role in blood coagulation.

Supplementary Material

Refer to Web version on PubMed Central for supplementary material.

Acknowledgements

The authors thank Betty Shen from the Fred Hutchinson Cancer Research Center for assistance with data processing and the SIBYLS beamline 12.3.1 at the Advanced Light Source for data collection access. This work was supported by the Dreyfus Foundation [Henry Dreyfus Teacher-Scholar Award], National Science Foundation [MRI 1429164], The Arlan Norman Award for Excellence in Student Mentoring and National Institutes of Health/National Heart, Lung and Blood Institute [award numbers R15 HL103518 and U54HL141981] to PCS and National Institutes of Health/National Heart, Lung and Blood Institute [award numbers R44HL117511, R44HL110448, U54HL112309 and U54HL141981 to CBD, HTS and PL].

References

1. Davie EW, Fujikawa K, Kisiel W. The coagulation cascade: initiation, maintenance, and regulation. Biochemistry. 1991;30(43):10363–10370. [PubMed: 1931959]
2. Davie EW. Biochemical and molecular aspects of the coagulation cascade. Thromb Haemost. 1995;74(1):1–6. [PubMed: 8578439]
3. van Dieijen G, Tans G, Rosing J, Hemker HC. The role of phospholipid and factor VIIIa in the activation of bovine factor X. J Biol Chem. 1981;256(7):3433–3442. [PubMed: 6782101]
4. Lenting PJ, van Mourik JA, Mertens K. The life cycle of coagulation factor VIII in view of its structure and function. Blood. 1998;92(11):3983–3996. [PubMed: 9834200]
5. Jankowski MA, Patel H, Rouse JC, Marzilli LA, Weston SB, Sharpe PJ. Defining 'full-length' recombinant factor VIII: a comparative structural analysis. Haemophilia. 2007;13(1):30–37. [PubMed: 17212722]
6. Eaton D, Rodriguez H, Vehar GA. Proteolytic processing of human factor VIII. Correlation of specific cleavages by thrombin, factor Xa, and activated protein C with activation and inactivation of factor VIII coagulant activity. Biochemistry. 1986;25(2):505–512. [PubMed: 3082357]
7. Lollar P, Hill-Eubanks DC, Parker CG. Association of the factor VIII light chain with von Willebrand factor. J Biol Chem. 1988;263(21):10451–10455. [PubMed: 3134349]
8. Vlot AJ, Koppelman SJ, Meijers JC, et al. Kinetics of factor VIII-von Willebrand factor association. Blood. 1996;87(5):1809–1816. [PubMed: 8634427]

Author Manuscript Author Manuscript Author Manuscript Author Manuscript

9. Hoffman M, Monroe DM, 3rd. A cell-based model of hemostasis. Thromb Haemost. 2001;85(6): 958–965. [PubMed: 11434702]
10. Hill-Eubanks DC, Parker CG, Lollar P. Differential proteolytic activation of factor VIII-von Willebrand factor complex by thrombin. Proc Natl Acad Sci U S A. 1989;86(17):6508–6512. [PubMed: 2505252]
11. Lollar P, Parker CG. Subunit structure of thrombin-activated porcine factor VIII. Biochemistry. 1989;28(2):666–674. [PubMed: 2496750]
12. Aly AM, Hoyer LW. Factor VIII-East Hartford (arginine 1689 to cysteine) has procoagulant activity when separated from von Willebrand factor. J Clin Invest. 1992;89(5):1382–1387. [PubMed: 1569181]
13. Pittman DD, Kaufman RJ. Proteolytic requirements for thrombin activation of anti-hemophilic factor (factor VIII). Proc Natl Acad Sci U S A. 1988;85(8):2429–2433. [PubMed: 3128786]
14. Regan LM, Fay PJ. Cleavage of factor VIII light chain is required for maximal generation of factor VIIIa activity. J Biol Chem. 1995;270(15):8546–8552. [PubMed: 7721754]
15. Shima M, Ware J, Yoshioka A, Fukui H, Fulcher CA. An arginine to cysteine amino acid substitution at a critical thrombin cleavage site in a dysfunctional factor VIII molecule. Blood. 1989;74(5):1612–1617. [PubMed: 2506948]
16. Brison CM, Mullen SM, Wuerth ME, et al. The 1.7 A X-ray crystal structure of the porcine factor VIII C2 domain and binding analysis to anti-human C2 domain antibodies and phospholipid surfaces. PLoS One. 2015;10(3):e0122447. [PubMed: 25775247]
17. Gilbert GE, Kaufman RJ, Arena AA, Miao H, Pipe SW. Four hydrophobic amino acids of the factor VIII C2 domain are constituents of both the membrane-binding and von Willebrand factor-binding motifs. J Biol Chem. 2002;277(8):6374–6381. [PubMed: 11698391]
18. Lu J, Pipe SW, Miao H, Jacquemin M, Gilbert GE. A membrane-interactive surface on the factor VIII C1 domain cooperates with the C2 domain for cofactor function. Blood. 2011;117(11):3181–3189. [PubMed: 21156843]
19. Meems H, Meijer AB, Cullinan DB, Mertens K, Gilbert GE. Factor VIII C1 domain residues Lys 2092 and Phe 2093 contribute to membrane binding and cofactor activity. Blood. 2009;114(18): 3938–3946. [PubMed: 19687511]
20. Pratt KP, Shen BW, Takeshima K, Davie EW, Fujikawa K, Stoddard BL. Structure of the C2 domain of human factor VIII at 1.5 A resolution. Nature. 1999;402(6760):439–442. [PubMed: 10586887]
21. Shen BW, Spiegel PC, Chang CH, et al. The tertiary structure and domain organization of coagulation factor VIII. Blood. 2008;111(3):1240–1247. [PubMed: 17965321]
22. Spiegel PC Jr., Jacquemin M, Saint-Remy JM, Stoddard BL, Pratt KP. Structure of a factor VIII C2 domain-immunoglobulin G4kappa Fab complex: identification of an inhibitory antibody epitope on the surface of factor VIII. Blood. 2001;98(1):13–19. [PubMed: 11418455]
23. Walter JD, Werther RA, Brison CM, et al. Structure of the factor VIII C2 domain in a ternary complex with 2 inhibitor antibodies reveals classical and nonclassical epitopes. Blood. 2013;122(26):4270–4278. [PubMed: 24085769]
24. Ngo JC, Huang M, Roth DA, Furie BC, Furie B. Crystal structure of human factor VIII: implications for the formation of the factor IXa-factor VIIIa complex. Structure. 2008;16(4):597–606. [PubMed: 18400180]
25. Parmenter CD, Stoilova-McPhie S. Binding of recombinant human coagulation factor VIII to lipid nanotubes. FEBS Lett. 2008;582(12):1657–1660. [PubMed: 18435924]
26. Stoilova-McPhie S, Lynch GC, Ludtke S, Pettitt BM. Domain organization of membrane-bound factor VIII. Biopolymers. 2013;99(7):448–459. [PubMed: 23616213]
27. Stoilova-McPhie S, Villoutreix BO, Mertens K, Kemball-Cook G, Holzenburg A. 3-Dimensional structure of membrane-bound coagulation factor VIII: modeling of the factor VIII heterodimer within a 3-dimensional density map derived by electron crystallography. Blood. 2002;99(4):1215–1223. [PubMed: 11830468]
28. Key NS, Negrier C. Coagulation factor concentrates: past, present, and future. Lancet. 2007;370(9585):439–448. [PubMed: 17679021]

Author Manuscript Author Manuscript Author Manuscript Author Manuscript

29. Allain JP, Frommel D. Antibodies to factor VIII. V. Patterns of immune response to factor VIII in hemophilia A. Blood. 1976;47(6):973–982. [PubMed: 1276479]
30. Bray GL, Gomperts ED, Courter S, et al. A multicenter study of recombinant factor VIII (recombinate): safety, efficacy, and inhibitor risk in previously untreated patients with hemophilia A. The Recombinate Study Group. Blood. 1994;83(9):2428–2435. [PubMed: 8167332]
31. Lusher JM, Lee CA, Kessler CM, Bedrosian CL, ReFacto Phase 3 Study G. The safety and efficacy of B-domain deleted recombinant factor VIII concentrate in patients with severe haemophilia A. Haemophilia. 2003;9(1):38–49.
32. Hay CR, Ludlam CA, Colvin BT, et al. Factor VIII inhibitors in mild and moderate-severity haemophilia A. UK Haemophilia Centre Directors Organisation. Thromb Haemost. 1998;79(4): 762–766. [PubMed: 9569189]
33. Brackmann HH, Gormsen J. Massive factor-VIII infusion in haemophiliac with factor-VIII inhibitor, high responder. Lancet. 1977;2(8044):933. [PubMed: 72276]
34. Doering C, Parker ET, Healey JF, Craddock HN, Barrow RT, Lollar P. Expression and characterization of recombinant murine factor VIII. Thromb Haemost. 2002;88(3):450–458. [PubMed: 12353075]
35. Doering CB, Healey JF, Parker ET, Barrow RT, Lollar P. High level expression of recombinant porcine coagulation factor VIII. J Biol Chem. 2002;277(41):38345–38349. [PubMed: 12138172]
36. Zakas PM, Gangadharan B, Almeida-Porada G, Porada CD, Spencer HT, Doering CB. Development and characterization of recombinant ovine coagulation factor VIII. PLoS One. 2012;7(11):e49481. [PubMed: 23152911]
37. Lollar P, Parker CG. pH-dependent denaturation of thrombin-activated porcine factor VIII. J Biol Chem. 1990;265(3):1688–1692. [PubMed: 2295651]
38. Lollar P, Parker ET, Fay PJ. Coagulant properties of hybrid human/porcine factor VIII molecules. J Biol Chem. 1992;267(33):23652–23657. [PubMed: 1429706]
39. Lillicrap D, Schiviz A, Apostol C, et al. Porcine recombinant factor VIII (Obizur; OBI-1; BAX801): product characteristics and preclinical profile. Haemophilia. 2016;22(2):308–317. [PubMed: 26278557]
40. Doering CB, Healey JF, Parker ET, Barrow RT, Lollar P. Identification of porcine coagulation factor VIII domains responsible for high level expression via enhanced secretion. J Biol Chem. 2004;279(8):6546–6552. [PubMed: 14660593]
41. Brown HC, Wright JF, Zhou S, et al. Bioengineered coagulation factor VIII enables long-term correction of murine hemophilia A following liver-directed adeno-associated viral vector delivery. Mol Ther Methods Clin Dev. 2014;1:14036. [PubMed: 26015976]
42. Brown HC, Zakas PM, George SN, Parker ET, Spencer HT, Doering CB. Target-Cell-Directed Bioengineering Approaches for Gene Therapy of Hemophilia A. Mol Ther Methods Clin Dev. 2018;9:57–69. [PubMed: 29552578]
43. Doering CB, Denning G, Dooriss K, et al. Directed engineering of a high-expression chimeric transgene as a strategy for gene therapy of hemophilia A. Mol Ther. 2009;17(7):1145–1154. [PubMed: 19259064]
44. Doering CB, Denning G, Shields JE, et al. Preclinical Development of a Hematopoietic Stem and Progenitor Cell Bioengineered Factor VIII Lentiviral Vector Gene Therapy for Hemophilia A. Hum Gene Ther. 2018;29(10):1183–1201. [PubMed: 30160169]
45. Spencer HT, Denning G, Gautney RE, et al. Lentiviral vector platform for production of bioengineered recombinant coagulation factor VIII. Mol Ther. 2011;19(2):302–309. [PubMed: 21081907]
46. Zakas PM, Brown HC, Knight K, et al. Enhancing the pharmaceutical properties of protein drugs by ancestral sequence reconstruction. Nat Biotechnol. 2017;35(1):35–37. [PubMed: 27669166]
47. Brown HC, Gangadharan B, Doering CB. Enhanced biosynthesis of coagulation factor VIII through diminished engagement of the unfolded protein response. J Biol Chem. 2011;286(27): 24451–24457. [PubMed: 21606503]
48. Svensson LA, Thim L, Olsen OH, Nicolaisen EM. Evaluation of the metal binding sites in a recombinant coagulation factor VIII identifies two sites with unique metal binding properties. Biol Chem. 2013;394(6):761–765. [PubMed: 23435097]

Author Manuscript Author Manuscript Author Manuscript Author Manuscript

49. Winn MD, Ballard CC, Cowtan KD, et al. Overview of the CCP4 suite and current developments. Acta Crystallogr D Biol Crystallogr. 2011;67(Pt 4):235–242. [PubMed: 21460441]
50. McCoy AJ, Grosse-Kunstleve RW, Adams PD, Winn MD, Storoni LC, Read RJ. Phaser crystallographic software. J Appl Crystallogr. 2007;40(Pt 4):658–674. [PubMed: 19461840]
51. Adams PD, Afonine PV, Bunkoczi G, et al. PHENIX: a comprehensive Python-based system for macromolecular structure solution. Acta Crystallogr D Biol Crystallogr. 2010;66(Pt 2):213–221. [PubMed: 20124702]
52. Jurrus E, Engel D, Star K, et al. Improvements to the APBS biomolecular solvation software suite. Protein Sci. 2018;27(1):112–128. [PubMed: 28836357]
53. Lyskov S, Gray JJ. The RosettaDock server for local protein-protein docking. Nucleic Acids Res. 2008;36(Web Server issue):W233–238. [PubMed: 18442991]
54. Tagliavacca L, Moon N, Dunham WR, Kaufman RJ. Identification and functional requirement of Cu(I) and its ligands within coagulation factor VIII. J Biol Chem. 1997;272(43):27428–27434. [PubMed: 9341195]
55. Canis K, Anzengruber J, Garenaux E, et al. In-depth comparison of N-glycosylation of human plasma-derived factor VIII and different recombinant products: from structure to clinical implications. J Thromb Haemost. 2018.
56. Parker ET, Doering CB, Lollar P. A1 subunit-mediated regulation of thrombin-activated factor VIII A2 subunit dissociation. J Biol Chem. 2006;281(20):13922–13930. [PubMed: 16513639]
57. Pipe SW, Saenko EL, Eickhorst AN, Kemball-Cook G, Kaufman RJ. Hemophilia A mutations associated with 1-stage/2-stage activity discrepancy disrupt protein-protein interactions within the triplicated A domains of thrombin-activated factor VIIIa. Blood. 2001;97(3):685–691. [PubMed: 11157485]
58. Leong L, Sim D, Patel C, et al. Noncovalent stabilization of the factor VIII A2 domain enhances efficacy in hemophilia A mouse vascular injury models. Blood. 2015;125(2):392–398. [PubMed: 25331117]
59. Monaghan M, Wakabayashi H, Griffiths A, Wintermute J, Fay PJ. Enhanced factor VIIIa stability of A2 domain interface variants results from an increased apparent affinity for the A2 subunit. Results from an increased apparent affinity for the A2 subunit. Thromb Haemost. 2014;112(3): 495–502. [PubMed: 24899227]
60. Gale AJ, Pellequer JL. An engineered interdomain disulfide bond stabilizes human blood coagulation factor VIIIa. J Thromb Haemost. 2003;1(9):1966–1971. [PubMed: 12941038]
61. Monaghan M, Wakabayashi H, Griffiths AE, Fay PJ. Stabilizing interactions between D666-S1787 and T657-Y1792 at the A2–A3 interface support factor VIIIa stability in the blood clotting pathway. J Thromb Haemost. 2016;14(5):1021–1030. [PubMed: 26878264]
62. Wakabayashi H, Monaghan M, Fay PJ. Cofactor activity in factor VIIIa of the blood clotting pathway is stabilized by an interdomain bond between His281 and Ser524 formed in factor VIII. J Biol Chem. 2014;289(20):14020–14029. [PubMed: 24692542]
63. Parker ET, Lollar P. Contribution of A1 subunit residue Q316 in thrombin-activated factor VIII to A2 subunit dissociation. Biochemistry. 2007;46(34):9737–9742. [PubMed: 17676877]
64. Adams TE, Hockin MF, Mann KG, Everse SJ. The crystal structure of activated protein C-inactivated bovine factor Va: Implications for cofactor function. Proc Natl Acad Sci U S A. 2004;101(24):8918–8923. [PubMed: 15184653]
65. Bardelle C, Furie B, Furie BC, Gilbert GE. Membrane binding kinetics of factor VIII indicate a complex binding process. J Biol Chem. 1993;268(12):8815–8824. [PubMed: 8473326]
66. Wakabayashi H, Griffiths AE, Fay PJ. Factor VIII lacking the C2 domain retains cofactor activity in vitro. J Biol Chem. 2010;285(33):25176–25184. [PubMed: 20529839]
67. Cheng J, Geng F, Hu J, Lu J. Single-molecule measurement and bioinformatics analysis suggest a preferred orientation of human coagulation factor VIII on hydrophobic interfaces. Biophys Chem. 2019;248:9–15. [PubMed: 30901531]
68. Mutucumarana VP, Duffy EJ, Lollar P, Johnson AE. The active site of factor IXa is located far above the membrane surface and its conformation is altered upon association with factor VIIIa. A fluorescence study. J Biol Chem. 1992;267(24):17012–17021. [PubMed: 1512240]

Author Manuscript Author Manuscript Author Manuscript Author Manuscript

69. Pipe SW, Eickhorst AN, McKinley SH, Saenko EL, Kaufman RJ. Mild hemophilia A caused by increased rate of factor VIII A2 subunit dissociation: evidence for nonproteolytic inactivation of factor VIIIa in vivo. Blood. 1999;93(1):176–183. [PubMed: 9864159]

70. Batsuli G, Deng W, Healey JF, et al. High-affinity, noninhibitory pathogenic C1 domain antibodies are present in patients with hemophilia A and inhibitors. Blood. 2016;128(16):2055–2067. [PubMed: 27381905]

71. Markovitz RC, Healey JF, Parker ET, Meeks SL, Lollar P. The diversity of the immune response to the A2 domain of human factor VIII. Blood. 2013;121(14):2785–2795. [PubMed: 23349389]

72. Novakovic VA, Cullinan DB, Wakabayashi H, Fay PJ, Baleja JD, Gilbert GE. Membrane-binding properties of the Factor VIII C2 domain. Biochem J. 2011;435(1):187–196. [PubMed: 21210768]

73. Chiu PL, Bou-Assaf GM, Chhabra ES, et al. Mapping the interaction between factor VIII and von Willebrand factor by electron microscopy and mass spectrometry. Blood. 2015;126(8):935–938. [PubMed: 26065652]

74. Yee A, Oleskie AN, Dosey AM, et al. Visualization of an N-terminal fragment of von Willebrand factor in complex with factor VIII. Blood. 2015;126(8):939–942. [PubMed: 26065653]

75. Shiltagh N, Kirkpatrick J, Cabrita LD, et al. Solution structure of the major factor VIII binding region on von Willebrand factor. Blood. 2014;123(26):4143–4151. [PubMed: 24700780]

Author Manuscript Author Manuscript Author Manuscript Author Manuscript

Essentials

- Hemophilia A is treated with recombinant factor VIII, which is highly immunogenic and unstable.
- A bioengineered variant of factor VIII, ET3i, has improved expression, activity and stability.
- The crystal structure of ET3i was determined, showing conformational changes to the C2 domain.
- Improved structures of human factor VIII were determined based on the ET3i crystal structure.

Author Manuscript Author Manuscript Author Manuscript Author Manuscript

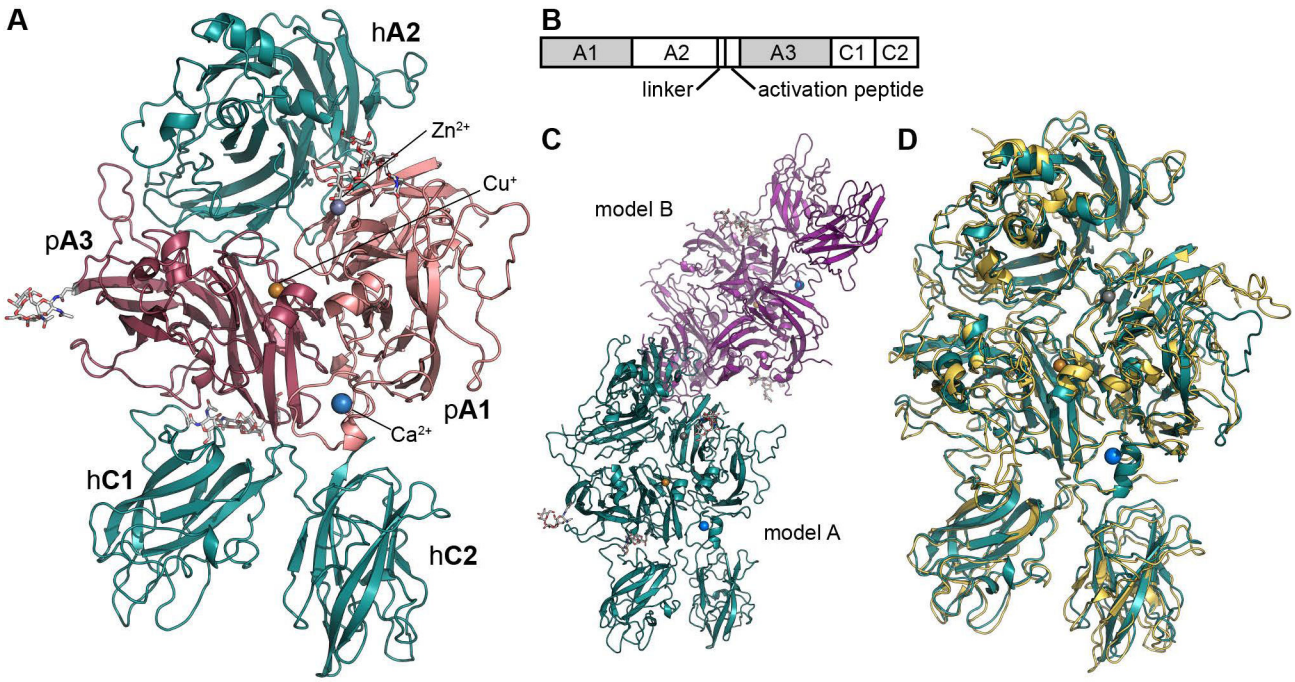

Figure 1. The structure of the bioengineered ET3i.

(A) Ribbon diagram representation of the ET3i A model (PDBID#: 6MF0, pink: porcine A1 domain, dark magenta: porcine A3 domain, dark teal: human A2, C1 and C2 domains). **(B)** Domain structure of ET3i (shaded region: porcine sequence, unshaded region: human sequence). **(C)** Asymmetric unit of ET3i. Two molecules are present within the asymmetric unit and modeled independently (dark teal: model A, purple: model B). **(D)** superposition of ET3i A model with the previous X-ray crystal structure of human FVIII (PDBID#: 2R7E, dark teal: ET3i A model, yellow: human FVIII).

Author Manuscript Author Manuscript Author Manuscript Author Manuscript

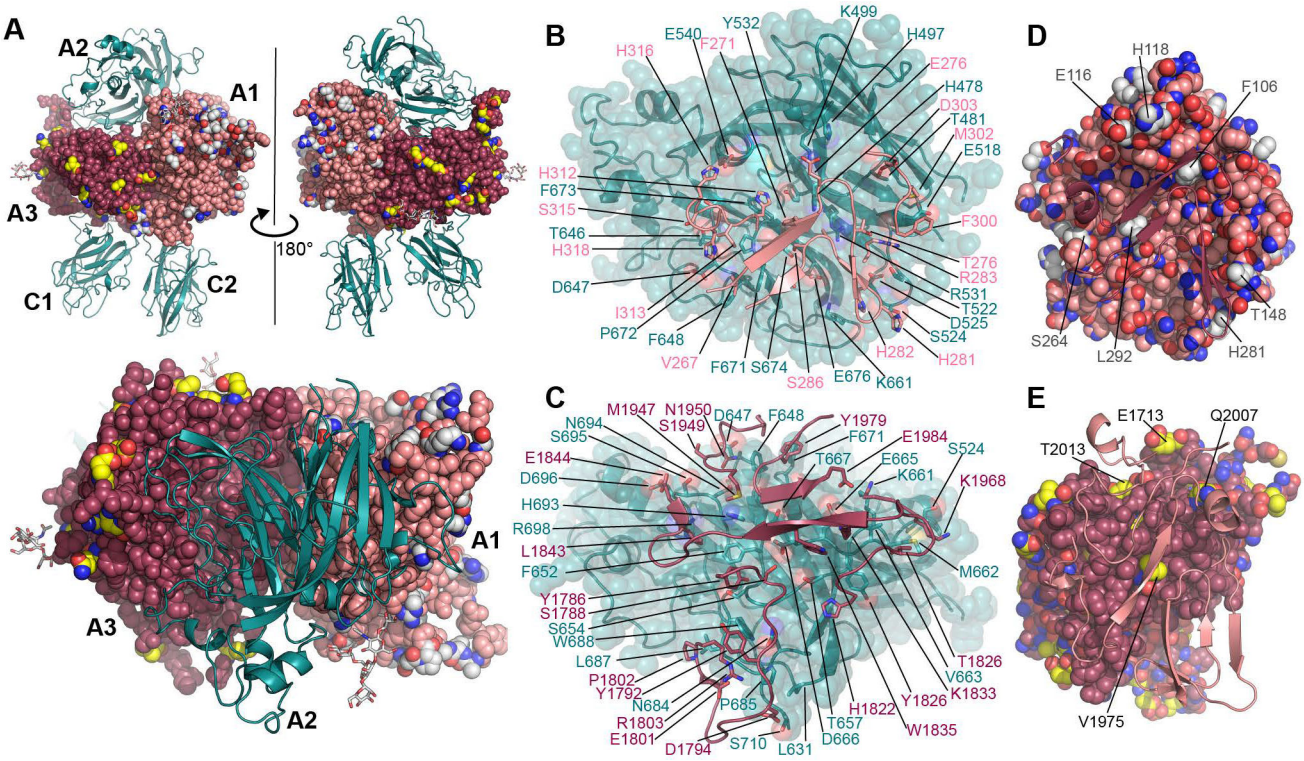

Figure 2. Factor VIII A domain interactions and human-ET3i sequence differences in ET3i.

(A) Crystal structure of ET3i highlighting the sequence differences for the A1 (pink VdW spheres) and A3 (dark magenta VdW spheres) domains. The residues that have different sequence between hFVIII and ET3i are highlighted (gray: A1 domain, yellow: A3 domain). **(B)** Detailed interfacial contacts between the A2 (dark teal) and A1 (pink) domains. **(C)** Detailed interfacial contacts between the A2 (dark teal) and A3(dark magenta) domains. **(D)** A1 domain sequence differences at the A1–A3 interface (same color scheme as (A)). **(E)** A3 domain sequence differences at the A1–A3 interface (same color scheme as (A)).

Author Manuscript Author Manuscript Author Manuscript Author Manuscript

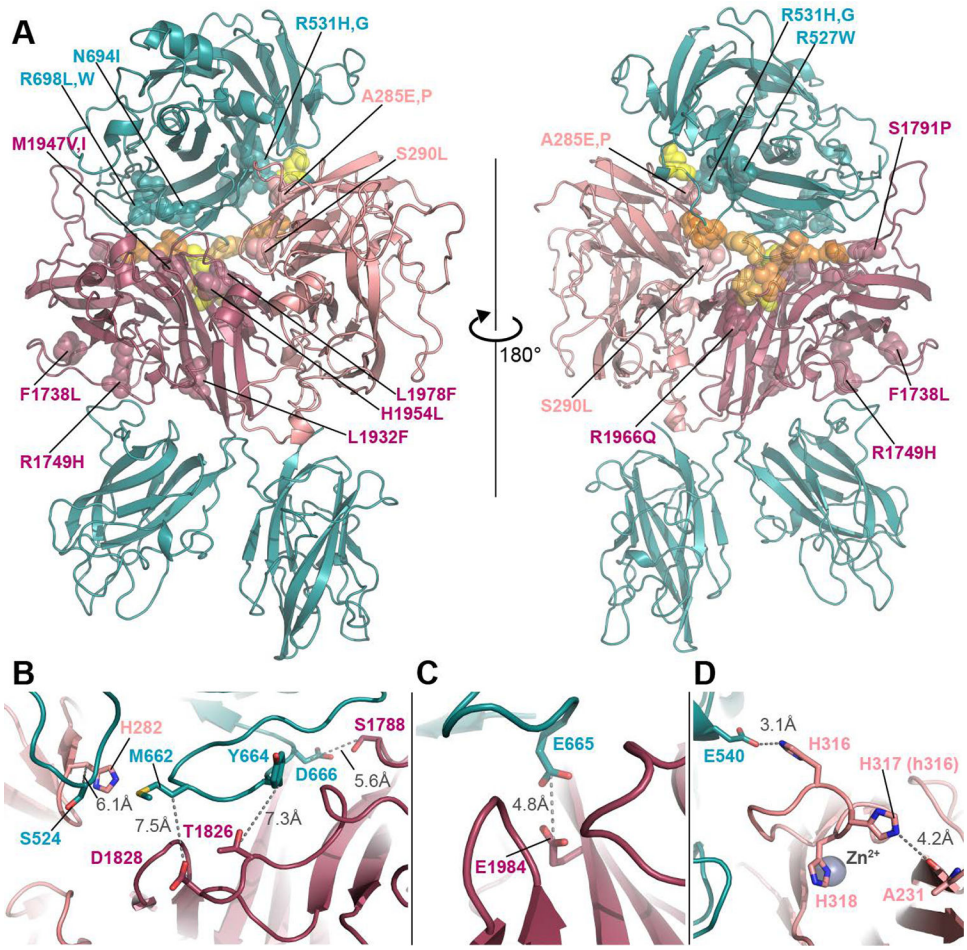

Figure 3. Hemophilia A-associated mutations and engineered sequence variances that affect A2 dissociation.

(A) Ribbon diagram representation of ET3i with hemophilia A mutations and engineered residue differences highlighted. Hemophilia A-associated mutations that result in lower activity for two-stage clotting assays versus one-stage are highlighted with specific mutations listed for the A1, A2 and A3 domains (pink, dark teal and dark magenta, respectively). Residues that increase hydrophobicity or introduce cysteines for disulfide bonds are also highlighted (yellow: hydrophobic residues, orange: cysteine residues). **(B)** Detailed packing representation of the A2 domain to highlight engineered cysteine residues for disulfide bond formation to stabilize the A2-bound state of FVIII. **(C)** Detailed packing representation of engineered hydrophobic residues to stabilize A2 binding. The mutations E1984A,V and E665I,V have been shown to increase FVIII clotting activity and A2 domain binding. **(D)** Packing representation of the A1–A2 interface near the Zn^{2+} binding site. The Q316H mutation in hFVIII decreases the dissociation rate constant for the A2 domain.

Author Manuscript Author Manuscript Author Manuscript Author Manuscript

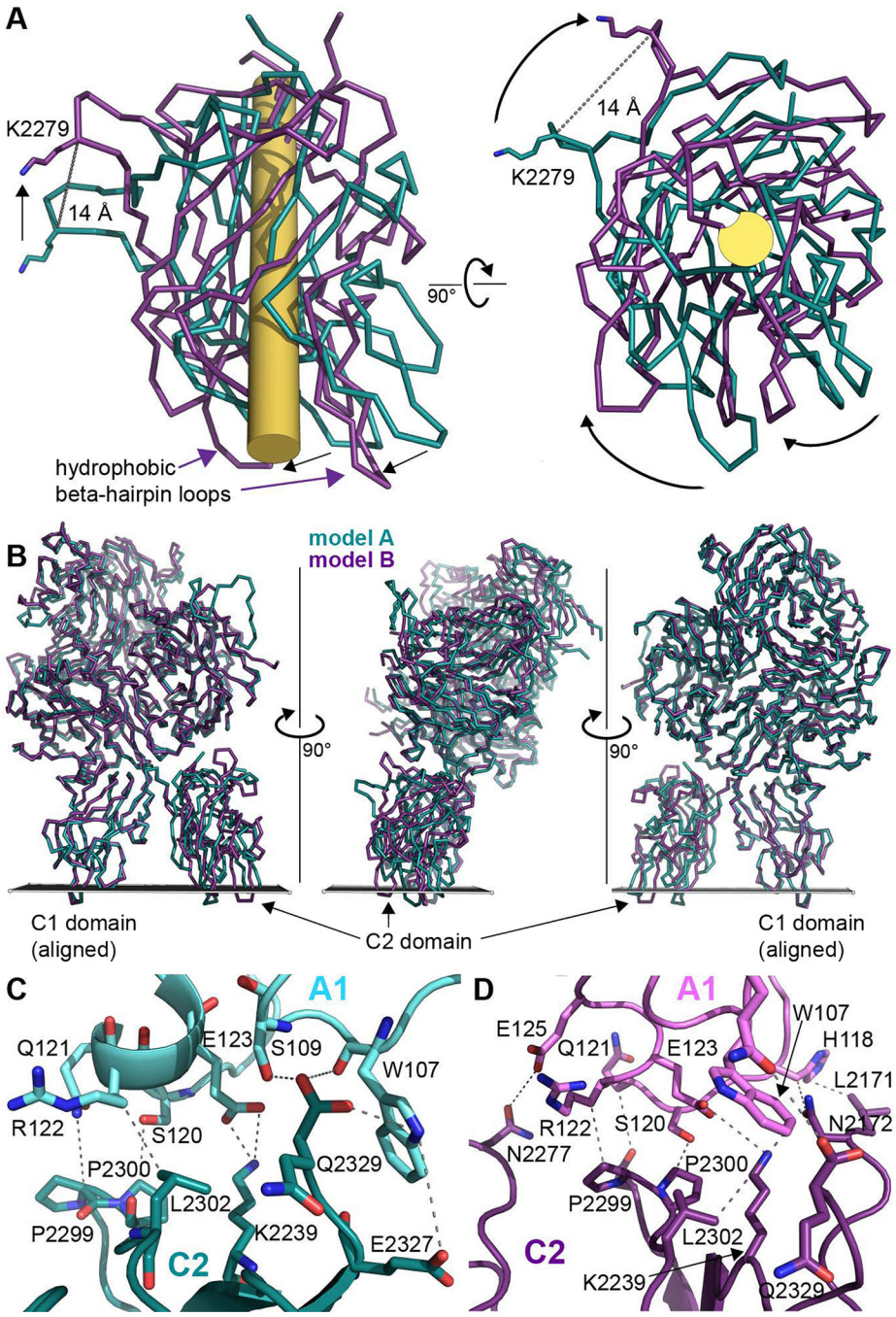

Figure 4. Conformational changes of the ET3i C2 domain.

(A) Detailed view of the C2 domain conformational changes. With the all-atom superposition of model A (dark teal) and model B (purple), the C2 domain rolls about a central axis (indicated by a cylinder highlighted in yellow) and tilts. **(B)** Projected membrane binding orientation of FVIII based on a previous model. For both models, the C1 domain is oriented into the plane of the membrane plane, illustrating the different conformations of the C2 domain. Model A (dark teal), model B (purple). **(C, D)** Interdomain interactions between the C2 and A1 domains for model A (C) and model B (D).

Author Manuscript Author Manuscript Author Manuscript Author Manuscript

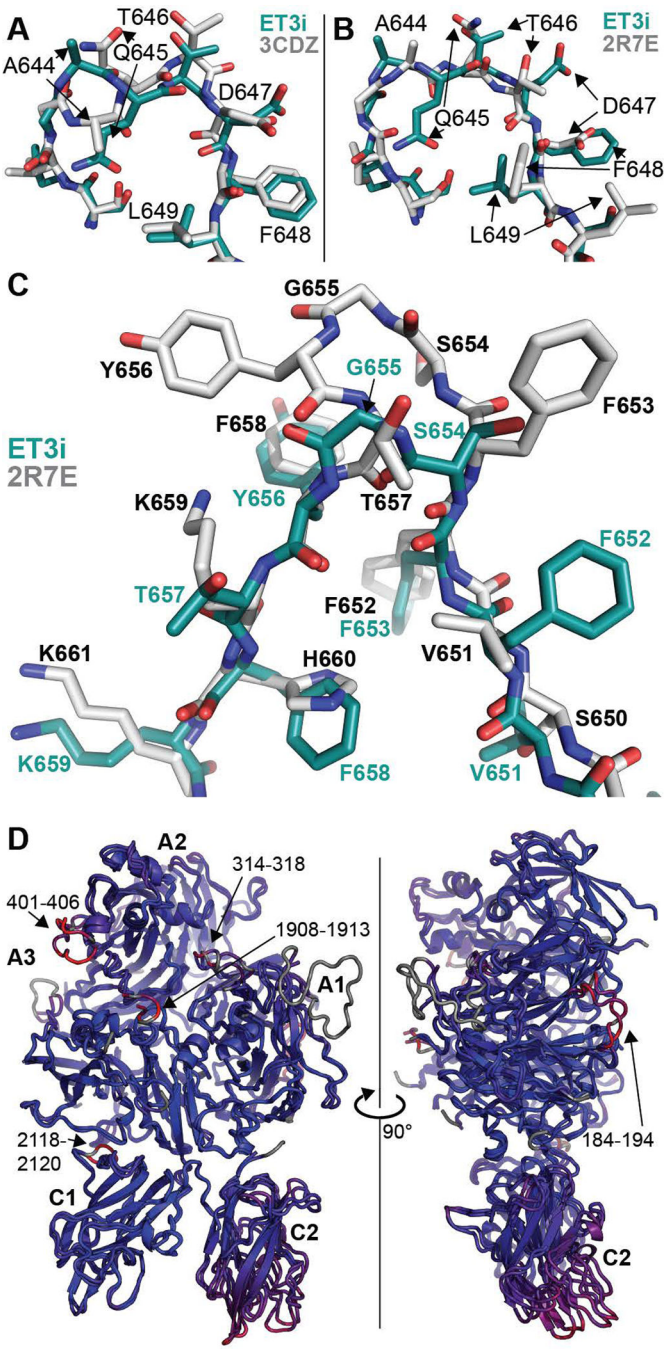

Figure 5. Structural differences between ET3i and previous hFVIII models, and the newly refined hFVIII structure.

(A, B) Stick diagram of the 644–648 loop of the A2 domain. Structural differences are observed for residues 644 and 645 between the 3.98 Å hFVIII structure (PDBID: 3CDZ) and ET3i (A), and for residues 645–649 between the 3.7 Å hFVIII structure (PDBID: 2R7E) and ET3i (B) (gray: hFVIII structures, dark teal: ET3i structure). **(C)** Stick diagram for the 651–659 loop of the A2 domain. In the 3.7Å structure, an extended loop was modeled, resulting in the amino acid mainchain being out-of-register by two amino acids, which propagates

Author Manuscript Author Manuscript Author Manuscript Author Manuscript

through the remainder of the A2 domain to residue 711. **(D)** Ribbon diagram representation and heat map of the structural superposition of ET3i (PDBID: 6MF0) with the newly refined hFVIII structure based on the previous 3.7 Å diffraction data (PDBID: 6MF2). Red: large RMSD regions, blue: low RMSD regions.

Author Manuscript Author Manuscript Author Manuscript Author Manuscript

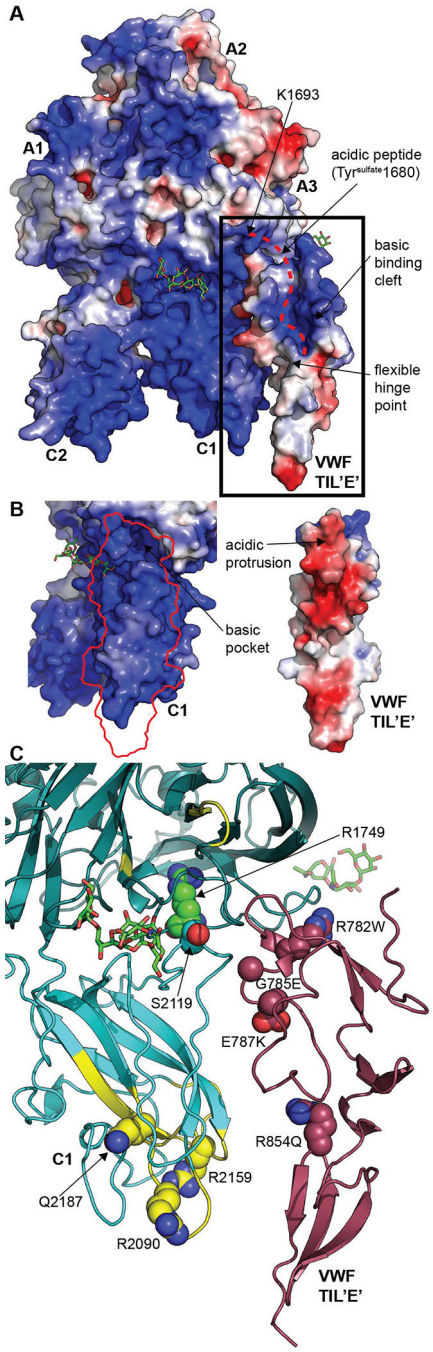

Figure 6: Modeling of the FVIII/VWF TIL'E' binding interface.

(A) Electrostatic potential surface representation of ET3i docked with the VWF TIL'E' domain (blue: positive charge, red: negative charge). The docking simulations were performed with Rosetta Docking on the ROSIE server, the surface potentials were calculated with APBS at surface potential values of ±5 kT/e, and the surfaces were displayed in PyMol. The dashed red line indicates the putative binding cleft for the acidic peptide on the N-terminus of the A3 domain. **(B)** Electrostatic potential surfaces of the interface between FVIII and the VWF TIL'E' domain. **(C)** Ribbon diagram representation of the FVIII/VWF

Author Manuscript Author Manuscript Author Manuscript Author Manuscript

TIL'E' interface. VdW spheres on FVIII representation hemophilia A-associated mutations that cause decreased VWF binding. VdW spheres on the TIL'E' domain represent Von Willebrand Disease Type 2N mutations, which cause loss of FVIII binding. Yellow ribbon representation indicates peptide regions that harbor H/D exchange protections upon binding to the VWF D'D3 domain (D' is also known as TIL'E').

Author Manuscript Author Manuscript Author Manuscript Author Manuscript

Table 1.

Data collection and refinement statistics.

X-ray data statistics (ET3i)	
Wavelength (Å)	0.977408
Resolution range (Å)	49.03 – 3.2 (3.314 – 3.2)
Space group	$P2_1$
Unit cell (Å)	a = 72.01 b = 135.86 c = 196.11 α = 90 β = 90.15 γ = 90
Total reflections	124688 (12388)
Unique reflections	62358 (6162)
Multiplicity	2.0 (2.0)
Completeness (%)	99.85 (99.31)
Mean I/sigma(I)	7.30 (1.29)
Wilson B-factor	62.63
R-merge	0.1098 (0.6483)
R-meas	0.1552 (0.9168)
R-pim	0.1098 (0.6483)
CC1/2	0.987 (0.542)
CC*	0.997 (0.838)
Model Refinement Statistics	
Reflections used in refinement	62287 (6162)
Reflections used for R-free	3077 (298)
R-work	0.2058 (0.3005)
R-free	0.2877 (0.3600)
CC(work)	0.938 (0.748)
CC(free)	0.867 (0.611)
Number of non-hydrogen atoms	20624
macromolecules	20233
ligands	385
solvent	6
Protein residues	2503
RMSD bonds (Å)	0.015
RMSD angles (°)	1.51
Ramachandran favored (%)	77.7
Ramachandran allowed (%)	14.37
Ramachandran outliers (%)	7.93
Rotamer outliers (%)	0.05
Clashscore	23.52
Average B-factor	61.42
macromolecules	60.27
ligands	122.14
solvent	33.3

Statistics for the highest-resolution shell are shown in parentheses.

Author Manuscript

Author Manuscript

Author Manuscript

Author Manuscript

Table 2.

ET3i-derived hFVIII model (6MF2) compared to previous datasets (2R7E, 3CDZ)

Model Refinement Statistics	6MF2 (2R7E data)	2R7E (3.7Å)	6MF2 (3CDZ data)	3CDZ (3.98Å)
R-work	0.252	0.279	0.262	0.256
R-free	0.284	0.347	0.295	0.327
Number of non-H atoms	10036	10985	10036	10317
Protein residues	1222	1512	1222	1438
RMSD (bonds)	0.51	0.5	0.34	0.68
RMSD (angles)	0.75	0.79	0.67	0.86
Ramachandran favored (%)	69.85	47	70.02	69
Ramachandran allowed (%)	21.1	26	20.84	20
Ramachandran outliers (%)	9.05	26	9.14	10
Rotamer outliers (%)	0	17	0	23
Clashscore	22.76	104	26.74	36
Average B-factor	53.27	168	160.74	199